Jami M. Gurley,[1] Olga Ilkayeva,[2] Robert M. Jackson,[1] Beth A. Griesel,[1] Phillip White,[2] Satochi Matsuzaki,[3] Rizwan Qaisar,[3] Holly Van Remmen,[3] Kenneth M. Humphries,[3] Christopher B. Newgard,[2] and Ann Louise Olson[1]

Enhanced GLUT4-Dependent Glucose Transport Relieves Nutrient Stress in Obese Mice Through Changes in Lipid and Amino Acid Metabolism

Diabetes 2016;65:3585–3597 | DOI: 10.2337/db16-0709

Impaired GLUT4-dependent glucose uptake is a contributing factor in the development of whole-body insulin resistance in obese patients and obese animal models. Previously, we demonstrated that transgenic mice engineered to express the human GLUT4 gene under the control of the human GLUT4 promoter (i.e., transgenic [TG] mice) are resistant to obesity-induced insulin resistance. A likely mechanism underlying increased insulin sensitivity is increased glucose uptake in skeletal muscle. The purpose of this study was to investigate the broader metabolic consequences of enhanced glucose uptake into muscle. We observed that the expression of several nuclear and mitochondrially encoded mitochondrial enzymes was decreased in TG mice but that mitochondrial number, size, and fatty acid respiration rates were unchanged. Interestingly, both pyruvate and glutamate respiration rates were decreased in TG mice. Metabolomics analyses of skeletal muscle samples revealed that increased GLUT4 transgene expression was associated with decreased levels of some tricarboxylic acid intermediates and amino acids, whereas the levels of several glucogenic amino acids were elevated. Furthermore, fasting acyl carnitines in obese TG mice were decreased, indicating that increased GLUT4-dependent glucose flux decreases nutrient stress by altering lipid and amino acid metabolism in skeletal muscle.

A major physiologic action of insulin is to promote the lowering of plasma glucose levels by increasing glucose uptake and storage in insulin-sensitive tissues. With insulin resistance and type 2 diabetes, the ability of insulin to stimulate glucose clearance is reduced. The deleterious effects of insulin resistance can result from hyperinsulinemia, hyperglycemia, or both. The overall therapeutic goal is to restore glucose tolerance and insulin sensitivity. Current therapies include strategies to increase insulin levels, decrease hepatic glucose output, increase insulin sensitivity in peripheral tissues, alter gastric function, or block renal glucose reabsorption (1). The appropriate approach for achieving this may vary according to the cause of disease, the stage of disease, or comorbidities. For example, increasing insulin levels through insulin injection or insulin secretagogues is associated with poor cardiovascular outcomes in obese patients (2). As the prevalence of obesity increases, more targets for enhancing glucose tolerance and insulin sensitivity are needed.

A promising target for improving glucose tolerance is glucose clearance by skeletal muscle. Skeletal muscle accounts for 70% of glucose clearance and has great capacity for insulin-independent glucose clearance through activity-dependent glucose uptake (3,4). We and other groups (5–10) have shown that transgenic (TG) overexpression of GLUT4 in adipose tissue alone, muscle alone, or all GLUT4-expressing tissues leads to improved glucose tolerance and reduced insulin levels in lean control and diabetic mice. However, the broader metabolic consequences of enhanced GLUT4-dependent glucose transport are not well understood. Insulin largely increases

[1]Department of Biochemistry & Molecular Biology, University of Oklahoma Health Sciences Center, Oklahoma City, OK
[2]Sarah W. Stedman Nutrition and Metabolism Center and Duke Molecular Physiology Institute, Departments of Pharmacology and Cancer Biology and Medicine, Duke University, Durham, NC
[3]Oklahoma Medical Research Foundation, Metabolism and Aging Program, Oklahoma City, OK

Corresponding author: Ann Louise Olson, ann-olson@ouhsc.edu.

Received 5 June 2016 and accepted 20 September 2016.

C.B.N. and A.L.O. are co-senior authors.

nonoxidative metabolism of glucose and increases glycogen synthesis (11). Insulin-dependent increases in nonoxidative glucose metabolism are tightly correlated with GLUT4 expression in muscle, indicating that GLUT4-dependent glucose flux is potentially limiting for this process. Although TG overexpression of GLUT4 increases glucose uptake, it does not increase the rate of glycogen synthesis in muscle (12,13). Because GLUT4 protein can mediate insulin-independent (i.e., activity-dependent) increases in glucose flux, we predict that enhanced GLUT4-dependent glucose flux may have insulin-independent effects on intermediary metabolism that improve glucose tolerance.

To better characterize the metabolic effects of GLUT4 overexpression, we used TG mice that moderately overexpress the human GLUT4 gene under the control of the human promoter, as previously described (14,15). This line of TG mice has two unique features that set it apart from other models. First, the level of overexpression is only twofold greater than the endogenous level of GLUT4 in skeletal muscle, which is similar to the increased expression that might be attained from a long-term exercise program. Second, the transgene is driven by a dynamic human promoter that allows the TG mouse to be subject to normal metabolic regulation. Herein, we report that GLUT4-dependent glucose flux reduces nutrient stress by altering the expression of key mitochondrial enzymes and by contributing to changes in amino acid and fatty acid metabolism in both lean and obese mice.

RESEARCH DESIGN AND METHODS

Animals and Diets

The animals used for these experiments were male C57BL/6 mice carrying a random insertion of the human GLUT4 gene (TG) have been described (14,16). Non-transgenic (NT) littermates served as controls. All procedures using animals were approved by the Institutional Animal Care and Use Committee at the University of Oklahoma Health Sciences Center.

Mice were kept in a temperature-controlled room with a 12-h light/dark cycle. Eight to 10 weeks after birth, the mice were housed in individual cages and were fed ad libitum either a chow diet (CD) (Purina) for lean mice or a high-fat diet (HFD) (60% kcal from fat, D12492; Research Diets, New Brunswick, NJ) for 5 weeks to induce obesity. The 5-week HFD feeding period was used to induce fasting hyperinsulinemia and fasting glycemia in wild-type mice raised in our facility (5). Experiments were performed in fasted and fed animals as indicated. Fasted animals had food removed overnight for 17 h prior to killing. Fed animals were those that received ad libitum feeding throughout the experimental period.

Mitochondrial Assays

Mitochondria were isolated from fresh gastrocnemius muscle from each leg, as previously described (17,18). Oxygen consumption measurements were obtained using a Clark-style oxygen sensing electrode system and recorded using NeoFox software (Instech Laboratories). Isolated skeletal muscle mitochondria were diluted to 250 ng/μL in buffer containing 1 mmol/L malate and either 1 mmol/L pyruvate or 25 μmol/L palmitoyl-DL-carnitine to initiate state 2 respiration. For glutamate respiration, 10 mmol/L glutamate only was used to initiate state 2 respiration. State 3 respiration was initiated by the addition of 0.25 mmol/L ADP. State 4 respiration began when exogenous ADP was completely converted to ATP.

Carboxylase-dependent respiration was estimated by measuring oxygen consumption as described above; however, tricarboxylic acid cycle (TCA) intermediates were provided by pyruvate plus $NaHCO_3$ (for pyruvate carboxylase [PC]) or propionyl carnitine plus $NaHCO_3$ (for propionyl CoA carboxylase [PCC]), as described previously (19).

The NADH-supported rate of superoxide anion production was measured as described previously (20,21). Briefly, the oxidation of hydroethidine by the fluorescent product 2-hydroxyethidium was measured with a spectrofluorometer (excitation 480 nm; emission 567 nm) using 10 μmol/L hydroethidine, 500 μmol/L NADH, and 50 μg of mitochondria. CuZn-SOD was used to verify that measurements were specific for superoxide anion. Values in the text are expressed as the rate of superoxide production versus the rate of NADH oxidase activity, as described previously (20).

Western Blot Analysis

Western blot analysis was performed with whole-cell detergent lysates that were prepared as previously described (5). Membranes were immunolabeled with anti–α/β-tubulin (catalog #2148; Cell Signaling Technology), anti–uncoupling protein 3 (UCP3) (catalog #ab3477; Abcam) anti–NADH dehydrogenase iron-sulfur protein 3 (NDUFS3) (catalog #459130; Invitrogen), anti–phospho-AMPKα T172 (catalog #2535; Cell Signaling Technology), anti-AMPKα (catalog #2603; Cell Signaling Technology), anti–phospho-4E-BP1 (catalog #2855; Cell Signaling Technology), anti–branched-chain ketoacid dehydrogenase (BCKDH) e1a (catalog #sc67200; Santa Cruz Biotechnology), anti-pSer293 BCKDH (catalog #ab200577; Abcam), anti–BCKDH kinase (#sc374425; Santa Cruz Biotechnology), anti-GLUT4 (catalog #sc1608; Santa Cruz Biotechnology), anti-slc38a2 (catalog #ab90677; Abcam), and a MitoBiogenesis Western Blot Cocktail ab123545 (Abcam) that was used to measure succinate dehydrogenase subunit A (SDHA) and cytochrome c oxidase subunit I. Rabbit anti–lipoic acid antibody for pyruvate dehydrogenase (PDH) subunit E2 and α-ketoglutarate (KG) dehydrogenase (α-KGDH) subunit E2 staining was provided by Kenneth Humphries (Oklahoma Medical Research Foundation, Oklahoma City, OK) (22). Membranes were visualized using the appropriate Alexa Fluor 680–conjugated secondary antibody and quantified using the Odyssey imaging system (LI-COR Biosciences). Alexa Fluor 680–conjugated streptavadin

(S32358; Life Technologies) was used to label and visualize biotin-containing PC and PCC.

Transmission Electron Microscopy

Gastrocnemius muscle blocks (1 mm^3) from lean NT and TG mice were fixed and processed as described previously (17). Sample preparation and microscopy were performed at the Oklahoma Medical Research Foundation Core Imaging Facility using a Hitachi H-7600 Transmission Electron Microscope at 80 kV. Initial inspection of electron micrographs was performed in blinded samples to test for genotype-specific differences in mitochondrial shape or distribution. Mitochondrial area in blinded samples was measured using National Institutes of Health ImageJ software.

Metabolomic Profile

Gastrocnemius muscles from lean and obese, NT and TG, fasted and fed mice were harvested and extracted in acetonitrile or perchloric acid (for malonyl CoA) at a final concentration of 50 mg wet weight of tissue/mL homogenate. The extracts were frozen at −80°C until further analysis. Amino acids, organic acids, acyl carnitines, and malonyl CoA were detected and quantified by mass spectrometry–based metabolic profiling performed as described previously (23,24). Raw metabolomic data are available upon request.

Muscle Glycogen, Triacylglycerol, and Carnitine Palmitoyltransferase-1 Assays

Gastrocnemius muscle glycogen was determined using the anthrone method (9). Lipids were extracted from gastrocnemius muscle by Folch extraction (5). Carnitine palmitoyltransferase-1 (CPT-1) activity was assayed in postnuclear lysates containing mitochondria processed from gastrocnemius skeletal muscle, as previously described (25).

Statistical Analysis

Data are expressed as the mean and SE. Data were analyzed by two-way ANOVA or Student *t* tests, as appropriate, using GraphPad Prism Software. Pairwise comparisons were made using least squares differences. Unless otherwise noted, significance was $P < 0.05$.

RESULTS

Effect of Enhanced GLUT4-Dependent Glucose Transport on Mitochondrial Structure and Function

To better understand the impact of increased GLUT4-dependent glucose flux, we measured the abundance of several key mitochondrial enzymes in insulin-responsive tissues via immunoblot detection (Fig. 1*A*). This included measurements for the following enzymes that participate in pyruvate metabolism, the TCA, and/or the electron transport chain: the E2 subunits of the PDH and α-KGDH complexes; PC; PCC; the nuclear-encoded NDUFS3 subunit of complex I; the nuclear-encoded SDHA and the mitochondrial-encoded cytochrome c oxidase I protein (COXI) of complex IV; UCP3; and tubulin as a loading control. These immunoblots were performed in whole-cell detergent extracts prepared from hindquarter skeletal muscle and perigonadal adipose tissue from lean NT and hGLUT4 TG mice. In skeletal muscle, all mitochondrial enzymes were reduced by ~50% in TG compared with NT mice, with the exception of PC and UCP3 (Fig. 1*B*). Extracts from perigonadal adipose tissue, a significantly less oxidative tissue, showed reduction in only COXI and PCC (Fig. 1*B*).

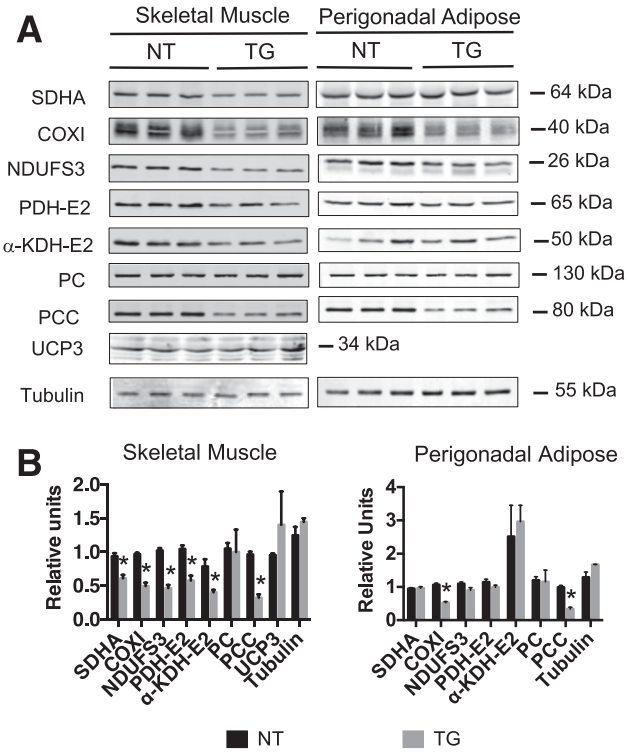

Figure 1—Expression of key mitochondrial enzymes in skeletal muscle and adipose tissue of hGLUT4 TG mice. *A*: Western blot analysis of three independent muscle samples measuring SDHA, COXI of complex IV, NDUFS3 subunit of complex I, E2 subunit of PDH (PDH-E2), E2 subunit of α-KGDH (α-KDH-E2), PC, PCC, UCP3, and tubulin. The samples were taken from NT mice fed a CD and hGLUT4 TG mice fed a CD. *B*: Western blot analysis histograms represented as the mean and SEM of the three independent samples. The asterisk (*) indicates the statistically significant difference ($P < 0.05$), as determined by two-tailed *t* test.

We next investigated whether the decreases in key mitochondrial enzymes were accompanied by decreases in mitochondrial number, mitochondrial area, or respiratory function. Mitochondrial number was estimated by measuring the ratio of mitochondrial DNA to nuclear DNA in hindquarter skeletal muscle. There was no significant difference in the ratio of mitochondrial DNA to genomic DNA in skeletal muscle between NT and TG mice (Fig. 2*A*). Mitochondrial morphology was observed using transmission electron microscopy, and representative images are shown in Fig. 2*B*. There were no observable differences in the size or appearance of mitochondria between genotypes. Mitochondrial function was determined by measuring basal (state 2) and ADP-dependent (state 3) respiration rates in isolated

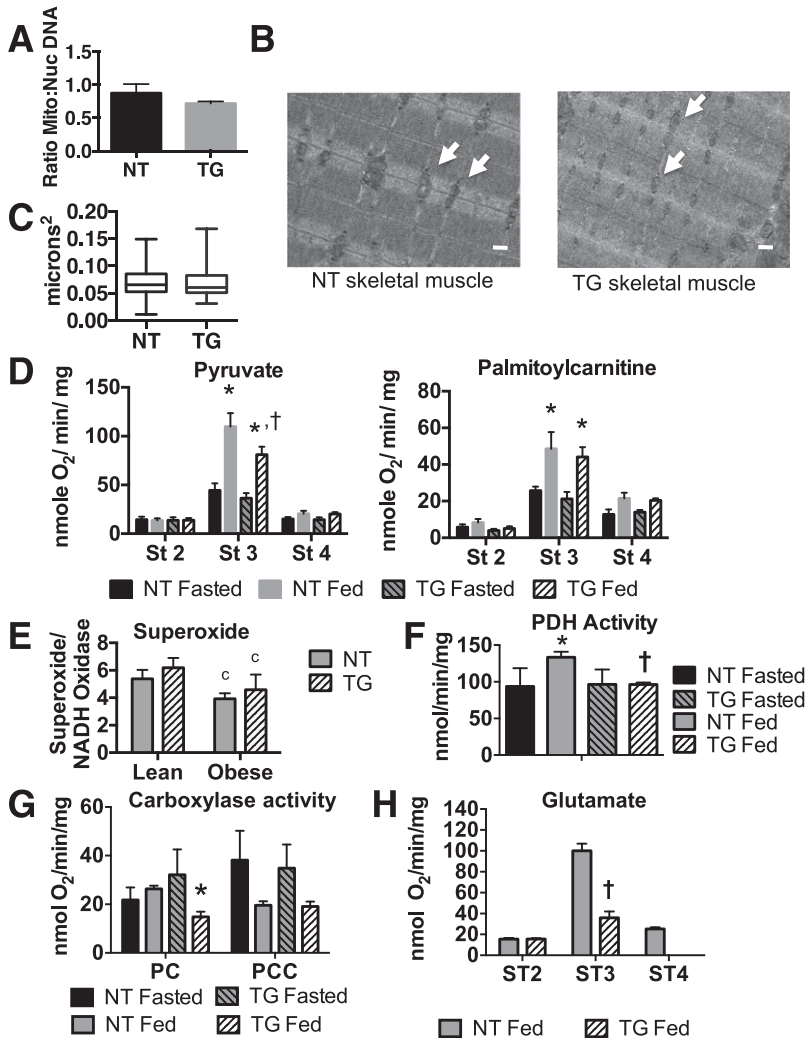

Figure 2—Skeletal muscle mitochondrial structure and function in NT mice fed a CD and hGLUT4 TG mice fed a CD. *A*: Ratio of mitochondrial (Mito) genomic DNA to nuclear (Nuc) DNA for CD-fed NT and TG mice. The data are the mean and SEM of three independent measurements. *B*: Electron micrographs of gastrocnemius skeletal muscle from CD-fed NT and TG mice. White arrowheads indicate examples of mitochondria. The white bar represents 500 nm. *C*: Box and whisker plot of mitochondrial area of 30 individual mitochondria from two NT and two TG mice. *D*: States 2, 3, and 4 respiration rates of pyruvate or palmitoylcarnitine from isolated mitochondria preparations from fasted and fed mice. *E*: Superoxide production unit of NADH oxidase activity in permeabilized mitochondria isolated from gastrocnemius muscle from CD-fed (lean) or 5-week HFD-fed (obese) mice. *F*: PDH from isolated mitochondria from fed and fasted mice. *G*: Pseudo-state 3 oxygen consumption rates for PC- and PCC-dependent respiration using pyruvate or acetyl carnitine and priopionyl carnitine, in the presence of ATP and stimulated with bicarbonate addition, from isolated mitochondria of fasted and fed NT and TG mice. *H*: States 2, 3, and 4 respiration rates for glutamate from isolated skeletal muscle mitochondria from fed NT and TG mice. The data are the mean and SEM of four independent experiments. The asterisk (*) indicates a significant difference comparing fasted and fed mice within a genotype ($P < 0.01$). The cross (†) indicates significant difference when comparing genotypes within a specific nutritional state ($P < 0.05$). The letter "c" indicates a significant difference when comparing lean and obese animals ($P < 0.01$). St/ST, state.

mitochondria from fasted or fed mice that were supplied with malate and either pyruvate or palmitoylcarnitine as substrates (Fig. 2*C*). Pyruvate respiration was significantly lower in mitochondria isolated from fed TG mice compared with fed NT mice; whereas, the TG had no impact on state 3 respiration of palmitoylcarnitine (Fig. 2*D*). In contrast, there were no genotype-specific differences in respiration rate using either set of substrates in mitochondria isolated from fasted animals. Interestingly, these data show that the TG-dependent decrease in mitochondrial enzymes did not result in a global decrease in mitochondrial respiration, but did result in a specific effect on pyruvate metabolism. Decreased pyruvate metabolism did not change the capacity for superoxide production in TG mice, although it was reduced in both genotypes during HFD feeding (Fig. 2*E*). To further investigate a TG-specific effect on pyruvate metabolism, PDH activity was measured in fasted and fed mitochondria. Consistent with mitochondrial respiration of pyruvate, PDH activity was decreased in fed TG mitochondria compared with NT mitochondria (Fig. 2*F*).

Because the ratio of PC to PCC protein was higher in TG mice, we hypothesized that pyruvate may be used preferentially for anaplerosis in TG mouse muscle. To investigate this, we performed carboxylase-dependent mitochondrial respiration studies in which TCA intermediates were derived either from pyruvate (via the PC pathway) or propionyl carnitine (via the PCC pathway). The rates of PC- and PCC-dependent respiration were not different between fasted NT and TG mice, indicating that the decreased expression of PCC did not decrease the ability of mitochondria to use propionyl CoA as an anaplerotic substrate in vitro (Fig. 2*G*). PC-dependent respiration was reduced in fed TG mice, which may reflect the decreased PDH activity seen under these conditions (Fig. 2*E*). Although these assays indicate that both pyruvate and propionyl CoA can be used for anaplerosis despite the relative TG-dependent decrease in PCC expression, they do not indicate which substrate is favored in vivo because the potential for allosteric regulation is eliminated.

Glutamate serves as another potential anaplerotic precursor. To test the ability of glutamate to support anaplerosis, we measured glutamate-dependent mitochondrial respiration in the absence of malate (Fig. 2*G*). State 2 respiration was not different between NT and TG mice; however, state 3 respiration was ~2.5× higher in NT mitochondria compared with TG mitochondria. Thus, glutamate is not a preferred substrate for respiration in fed TG mice and contributes minimally to anaplerosis.

To test the impact of GLUT4 overexpression on TCA intermediates, we used targeted gas chromatography/mass spectrometry to measure the concentrations of multiple organic acids in muscle samples from fasted and ad libitum–fed NT and TG mice in both lean and diet-induced obese mice. Obese mice were fed an HFD for 5 weeks, which was sufficient to increase body mass in both genotypes and fasting hyperglycemia in NT mice (5). The TG mice did not have the altered levels of the end products of glycolysis, pyruvate and lactate, seen in lean mice. Obesity significantly reduced steady-state levels of pyruvate in fasted and fed TG mice (Fig. 3), but not in NT mice. Citrate, the product of the initiating citrate synthase reaction of the TCA, was not changed by nutritional state (fasting or feeding), the presence of the TG, or obesity (Fig. 3). Consistent with reduced fed glutamate respiration (Fig. 2*G*), steady-state levels of α-KG were reduced in fed lean TG mice (Fig. 3). During fasting, α-KG levels in lean TG and lean NT mice were not different. Thus, the primary genotype-dependent difference in α-KG was that the fasting-to-fed increase was lost in lean TG mice. Obesity resulted in both a loss in the fasting-to-fed increase in α-KG in NT mice and a significant decrease in α-KG in fasted TG mice compared with their NT fasted counterparts.

Steady-state levels of the later TCA intermediates succinate, fumarate, and malate (products of equilibrium reactions) were generally reduced by ~50% in obese TG mice (Fig. 3). Succinate and malate were also reduced in lean TG mice compared with NT mice. Together, the TG-induced reduction in key mitochondrial enzymes (as well as decreased pyruvate- and glutamate-dependent anaplerosis) was correlated with a reduction in the concentrations of intermediates generated in the later stages of the TCA. This suggests that the rates of anaplerosis and cataplerosis were altered by either the presence of the TG and/or the stress of obesity.

Effect of Enhanced GLUT4-Dependent Glucose Transport on Branched-Chain Amino Acid Levels and Mammalian Target of Rapamycin Signaling

Although PCC activity in isolated mitochondria was not different between genotypes, this assay does not measure flux through the pathway. If decreased succinate is due to decreased PCC-dependent anaplerosis, we predicted that steady-state levels of branched-chain amino acids (BCAAs) would be increased. To test this, we measured the concentrations of BCAAs in skeletal muscle extracts and found that Val and Leu/Ile were increased in both lean and obese TG mice (Fig. 4*A*). To determine whether the increased BCAA levels were sufficient to activate mammalian target of rapamycin (mTOR) signaling, we measured the phosphorylation of 4E-BP1, a downstream target of mTOR signaling. As expected, the phosphorylation of 4E-BP1 was increased in the fed state in lean NT and TG mice (Fig. 4*B*). In obese NT mice, the transition from fasting to feeding was not accompanied by increased 4E-BP1 phosphorylation. The presence of the TG in obese mice restored the phosphorylation of 4E-BP1 in the fed state to the levels observed in lean controls (Fig. 4*B*). Because 4E-BP1 phosphorylation was not increased in fasted TG mice, we conclude that the levels of BCAAs were not high enough to activate the mTOR pathway. Our findings contrast with those of Herman et al. (7), who observed that adipose-specific overexpression of GLUT4 resulted in increased BCAA levels that were sufficient to activate basal mTOR signaling. It is not clear whether this discrepancy was due to a difference in the level of GLUT4 overexpression between the studies or whether the difference was tissue specific for adipose.

To investigate the mechanism for increased steady levels of BCAAs, we measured the abundance of phosphorylated and total BCKDH e1a (Fig. 4*B*). There was a significant increase in the ratio of phospho-BCKDH to total BCKDH in both lean and obese TG mice, which is consistent with the inactivation of BCAA degradation (Fig. 4*C*). Increased phospho-BCKDH expression was not due to the increased expression of BCKDH kinase (BDK), the enzyme responsible for phosphorylating BCKDH (Fig. 4*B*).

Effect of Enhanced GLUT4-Dependent Glucose Uptake on Glucogenic Amino Acid Metabolism

To begin to understand the specific fate of GLUT4-dependent glucose flux, we measured glycogen and glucogenic amino acid levels in skeletal muscle. As expected, glycogen levels were higher in fed than in fasted conditions in all genotypes (Fig. 6*A*). Glycogen levels in fasted and fed

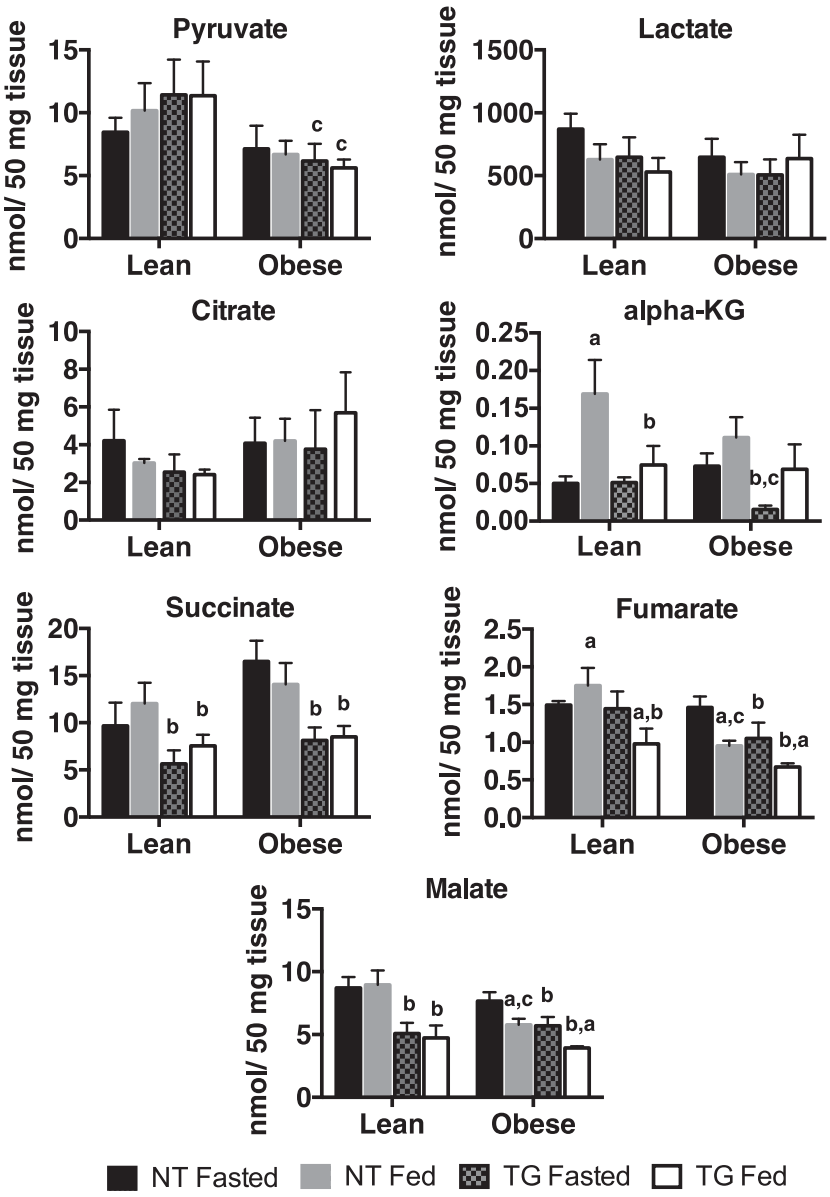

Figure 3—Metabolic organic acids in skeletal muscle of fasted and fed NT and TG lean (CD) and obese (HFD) mice. Data are the mean and SEM for five animals per group. Data were analyzed by two-way ANOVA. Pairwise comparisons of 95% CIs established significant differences ($P < 0.05$) between groups. The letter "a" designates a significant difference due to nutritional state (fasted or fed) for a given strain (NT or TG) or body mass (lean or obese). The letter "b" designates a significant difference due to strain for a given nutritional state or body mass. The letter "c" indicates a significant difference due to body mass for a given nutritional state or strain.

mice showed no TG-specific differences in either lean or obese mice. Obesity tended to lower fed glycogen levels; however, this decrease did not reach statistical significance ($P < 0.09$). These results suggest that increased GLUT4-dependent glucose transport is not rate limiting for muscle glycogen synthesis.

The presence of the TG significantly increased levels of the most abundant glucogenic amino acids, Ala and Gly, in skeletal muscle (Fig. 5*B*). Interestingly, the GLUT4 TG also significantly decreased Glu/Gln. These TG-dependent effects were most prominent in the fed state, when glucose flux is highest. Although obesity resulted in a significant reduction in Ala and Gly levels in the muscle of TG mice compared with that in their lean controls, the TG mice maintained Ala and Gly levels at significantly higher levels than their NT obese counterparts (Fig. 5*B*). Changes in amino acid levels were not a result of changes in system A amino acid transporter (slc38a2) expression (Fig. 5*C*). As shown previously, GLUT4 protein was increased in both lean and obese TG mouse skeletal muscle (Fig. 5*C*) (5). These data suggest that increased GLUT4-dependent glucose flux in TG animals significantly alters amino acid synthesis. Together, these data suggest that increased GLUT4-dependent glucose flux increases Ala and Gly

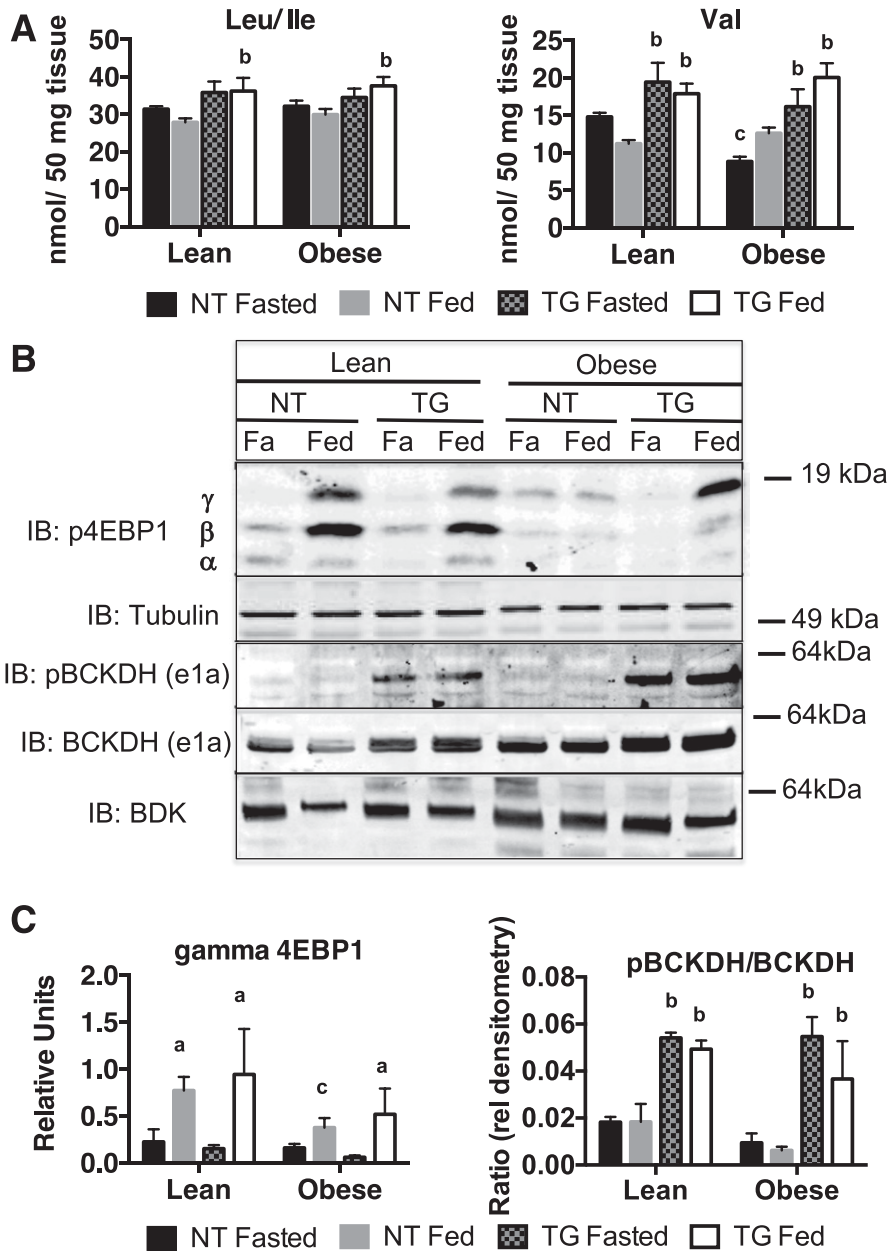

Figure 4—Skeletal muscle BCAAs and 4E-BP1 hyperphosphorylation in fasted (Fa) and fed NT and hGLUT4 TG mice fed a CD (Lean) or an HFD (Obese) for 5 weeks. *A*: BCAA data are the mean and SEM for five animals per group. *B*: Representative Western blot immunoblotted (IB) for 4E-BP1 hyperphosphorylation, phospho-BCKDH (pBCKDH) and total BCKDH e1a, and BDK from whole-cell skeletal muscle extracts. *C*: Quantification of hyperphosphorylated (γ) 4EBP1 and the ratio of phospho-BCKDH to total BCKDH. Data are the mean and SEM of the relative densitometry units for the analysis of three independent muscle extracts for each group. Data were analyzed by two-way ANOVA. Pairwise comparisons of 95% CIs established significant differences ($P < 0.05$) between groups. The letter "a" designates a significant difference due to nutritional state (fasted or fed) for a given strain (NT or TG) or body mass (Lean or Obese). The letter "b" designates a significant difference due to strain for a given nutritional state or body mass. The letter "c" indicates a significant difference due to body mass for a given nutritional state or strain.

synthesis at the expense of Glu/Gln synthesis and that the incoming glucose is being used for glucogenic amino acid synthesis, rather than anaplerosis. These data are consistent with the observations of decreased mitochondrial enzyme levels, PDH activity, levels of late-stage TCA intermediates, and pyruvate- and glutamine-dependent respiration in TG mice (Fig. 2*G*).

Less abundant amino acids were also differentially regulated by expression of the TG or obesity. For example, TG mice showed a significant increase in fed state Pro and Ser levels in skeletal muscles of both lean and obese animals, whereas Met levels were unchanged with feeding or the presence of the TG (Fig. 6). In contrast, obesity significantly reduced Met, Arg, and Pro levels in both

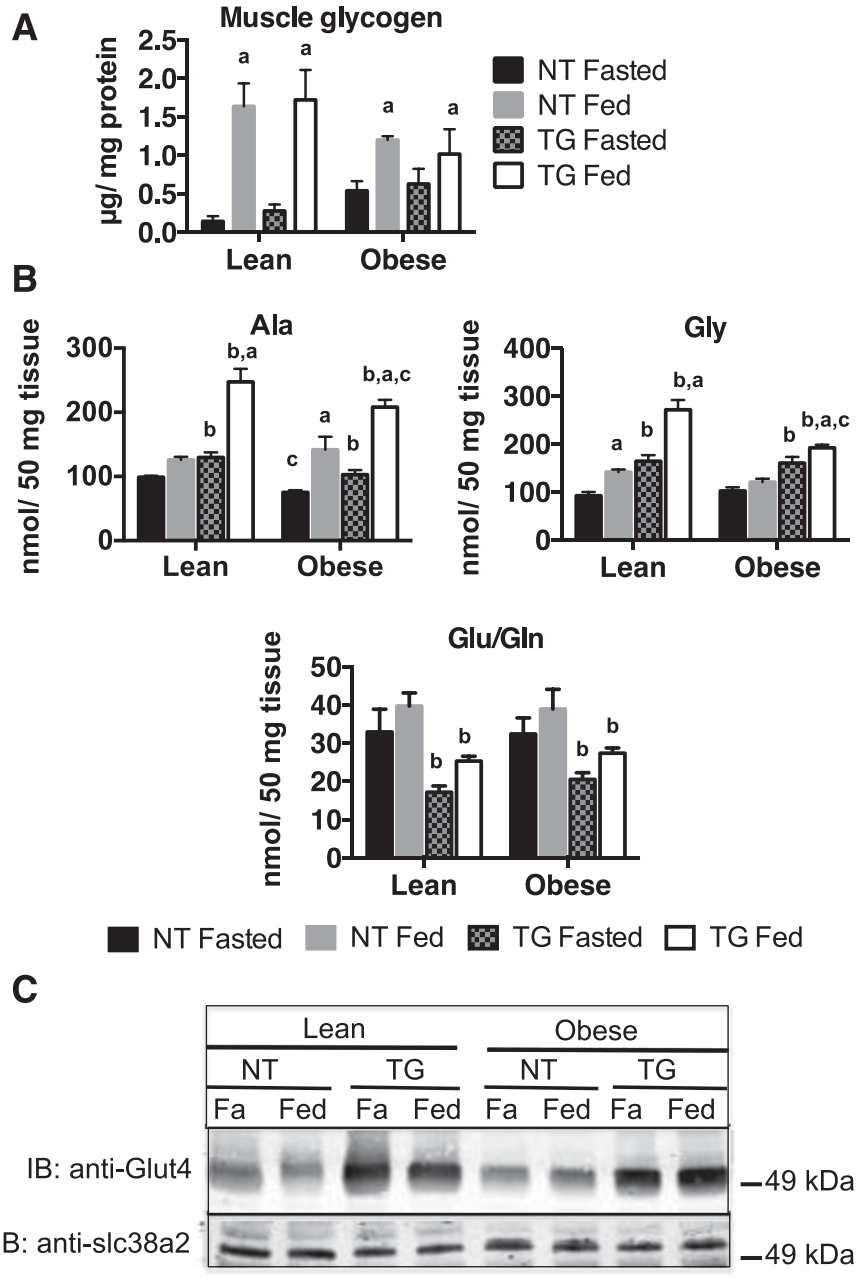

Figure 5—Skeletal muscle (*A*) glycogen and amino acids (*B*) Ala, Gly, and Glu/Gln in fasted (Fa) and fed NT and hGLUT4 TG mice fed a CD (Lean) or an HFD (Obese) for 5 weeks. Data are the mean and SEM for five animals per group. Data were analyzed by two-way ANOVA. Pairwise comparisons of 95% CIs established significant differences ($P < 0.05$) between groups. The letter "a" designates a significant difference due to nutritional state (fasted or fed) for a given strain (NT or TG) or body mass (Lean or Obese). The letter "b" designates a significant different due to strain for a given nutritional state or body mass. The letter "c" indicates a significant difference due to body mass for a given nutritional state or strain. *C*: Representative Western blots (n-3 independent sets) imunoblotted (IB) for GLUT4 and slc38a2 levels from whole-cell skeletal muscle extracts.

genotypes. In obese, fasted TG mice, Asp/Asn levels were significantly elevated over those of NT mice.

Effect of Enhanced GLUT4-Dependent Glucose Transport on Skeletal Muscle Acyl Carnitines, AMPK Signaling, and Triacylglycerides

Long-chain acyl carnitines (C18–C14) can accumulate when rates of fatty acid oxidation are reduced (26), but can also indicate increased influx and oxidation of fatty acids. The reduced TCA intermediates and the decreased expression of TCA and electron transport chain enzymes in TG mice predicted that the rate of fatty acid oxidation might be reduced in the TG animals. To test this, we measured the abundance of long-chain acyl carnitines in skeletal muscle. In fasted lean mice, the presence of the TG did not affect any of the long-chain acyl carnitines

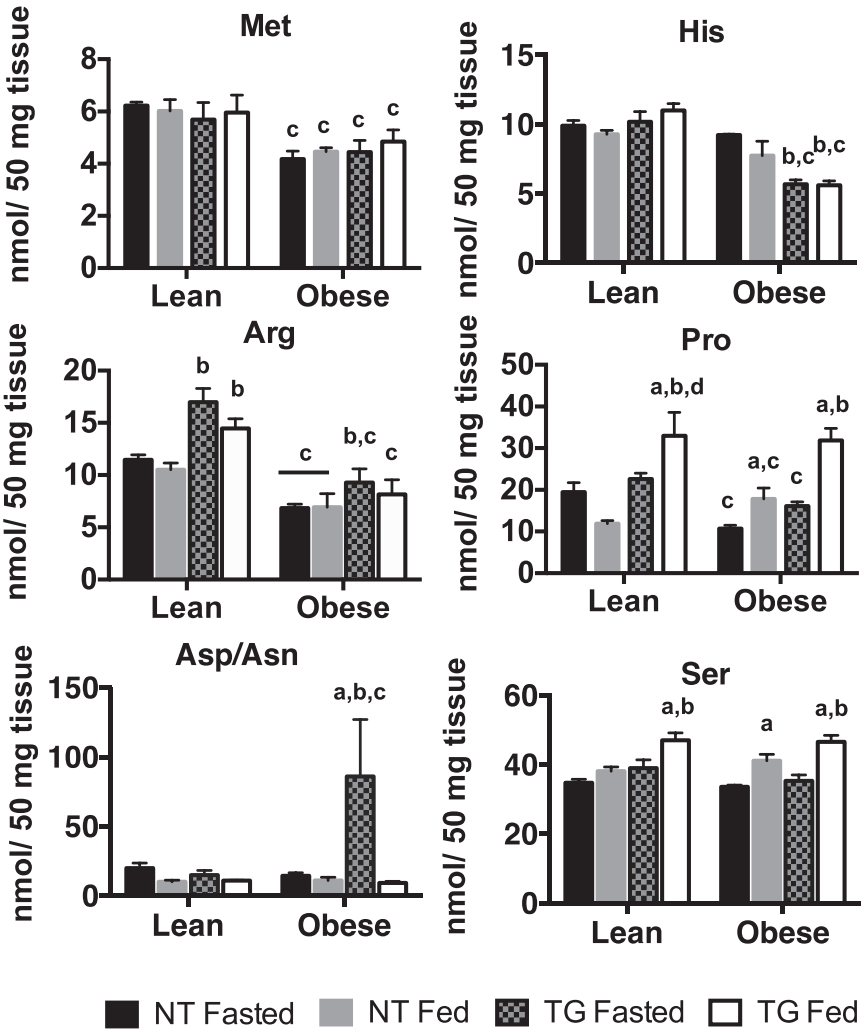

Figure 6—Amino acids in fasted and fed skeletal muscle of NT and hGLUT4 TG mice fed a CD (Lean) or an HFD (Obese) for 5 weeks. Data are the mean and SEM for five animals per group. Data were analyzed by two-way ANOVA. Pairwise comparisons of 95% CIs established significant differences ($P < 0.05$) between groups. The letter "a" designates a significant difference due to nutritional state (fasted or fed) for a given strain (NT or TG) or body mass (Lean or Obese). The letter "b" designates a significant different due to strain for a given nutritional state or body mass. The letter "c" indicates a significant difference due to body mass for a given nutritional state or strain.

measured (Fig. 7*A*). Fasted, obese NT mice showed a significant increase in long-chain acyl carnitines compared with their lean counterparts, and a decrease in these metabolites in the fed state (Fig. 7*A*). Interestingly, lean TG mice also showed a significant reduction in long-chain acyl carnitines in the fed state. Importantly, in contrast to NT mice, the TG mice did not show obesity-dependent increases in acyl carnitines in the fasted state (Fig. 7*A*). These data suggest that the TG mouse relieves nutrient stress by decreasing the accumulation of acyl carnitines that are produced as a result of diet-induced obesity.

Acetyl carnitine, a product of the carnitine acetyltransferase (CrAT) reaction, is generated as a means of buffering the free CoA (CoASH) pool in skeletal muscle mitochondria (27). Because CrAT mediates a thermodynamically favorable reaction, acetyl carnitine levels reflect the mitochondrial acetyl CoA and free carnitine pools. Acetyl carnitine levels were significantly higher in the fed state compared with the fasted state, regardless of genotype or body mass (Fig. 7*B*). This is expected because the fed state is a state of nutrient excess relative to fasting. Obesity slightly, but significantly, decreased fasting acetyl carnitine in NT mice, but not in TG mice (Fig. 7*B*). The fact that acetyl carnitine levels are very similar between NT and TG mice suggests that the production of acetyl CoA and free carnitine is similar in both genotypes. Thus, the accumulation of long-chain acyl carnitines with obesity and reduction of obesity-induced long-chain acyl carnitine levels with hGLUT4 overexpression is unlikely to be explained by differences in CrAT activity.

CPT-1 mediates the increased production of long-chain acyl carnitines in the fasted state. CPT-1 activity is suppressed

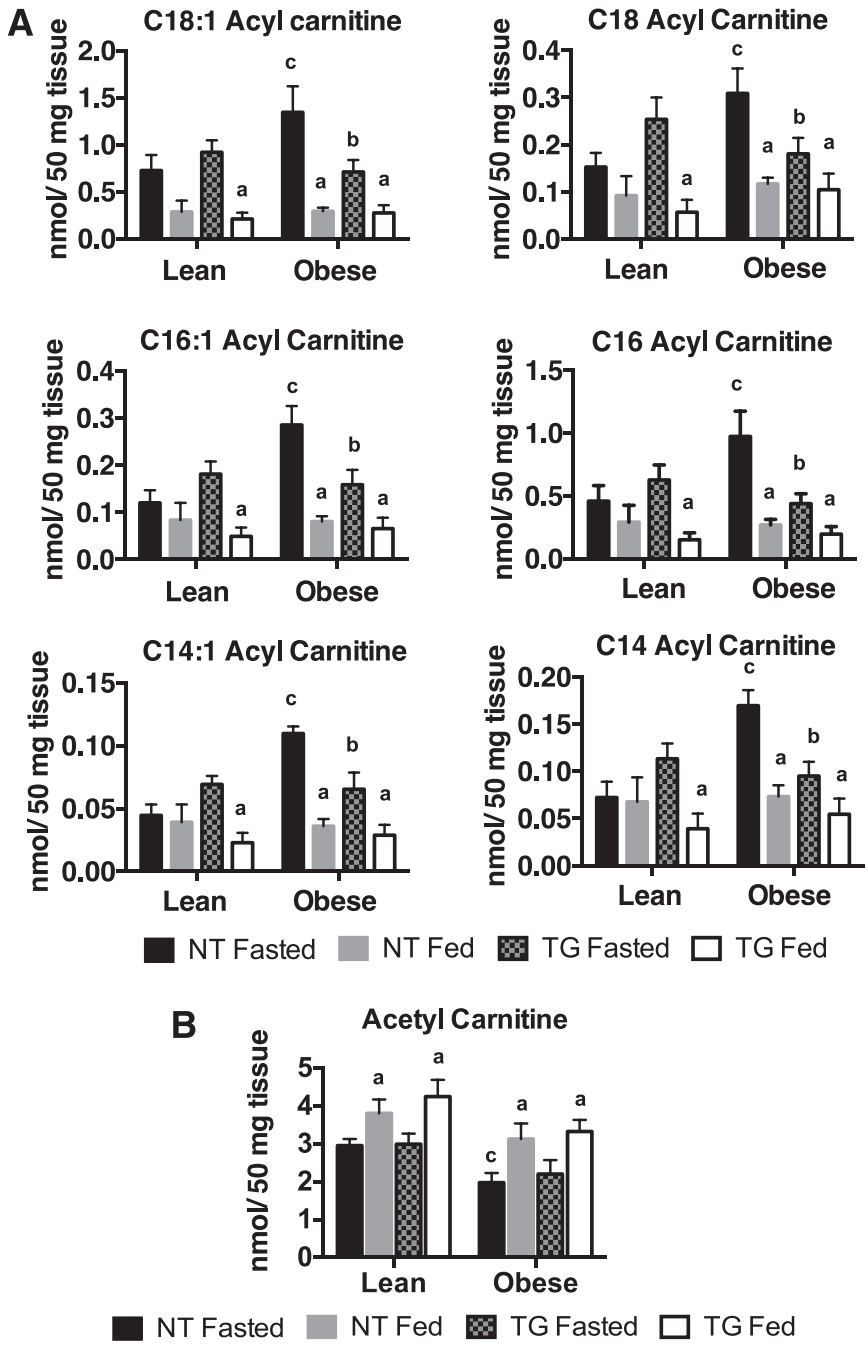

Figure 7—Long-chain acyl carnitines (*A*) and acetyl carnitine (*B*) in fasted and fed NT and hGLUT4 TG mice in skeletal muscle of mice fed a CD (Lean) or an HFD (Obese) for 5 weeks. Data are the mean and SEM for five animals per group. Data were analyzed by two-way ANOVA. Pairwise comparisons of 95% CIs established significant differences ($P < 0.05$) between groups. The letter "a" designates a significant difference due to nutritional state (fasted or fed) for a given strain (NT or TG) or body mass (Lean or Obese). The letter "b" designates a significant difference due to strain for a given nutritional state or body mass. The letter "c" indicates a significant difference due to body mass for a given nutritional state or strain.

by allosteric inhibition of malonyl CoA, a product of the acetyl CoA carboxylase reaction. To investigate the influence of obesity and the TG on AMPK signaling (which inhibits acetyl CoA carboxylase activity), we measured AMPKα phosphorylation on Thr172 as an indicator of the AMPK activation state. Phospho-AMPK was increased in fasted NT mice compared with fed NT mice in both lean and obese states (Fig. 8*A*). Although obesity increased fasting phospho-AMPK levels in both NT and TG mice relative to their lean counterparts, the presence of the TG significantly reduced fasting phospho-AMPK levels compared with those of NT mice. Total AMPK protein levels were not different between genotypes or diet (Fig. 8*A*). Reduced phospho-AMPK in obese, fasted TG mice did not lead

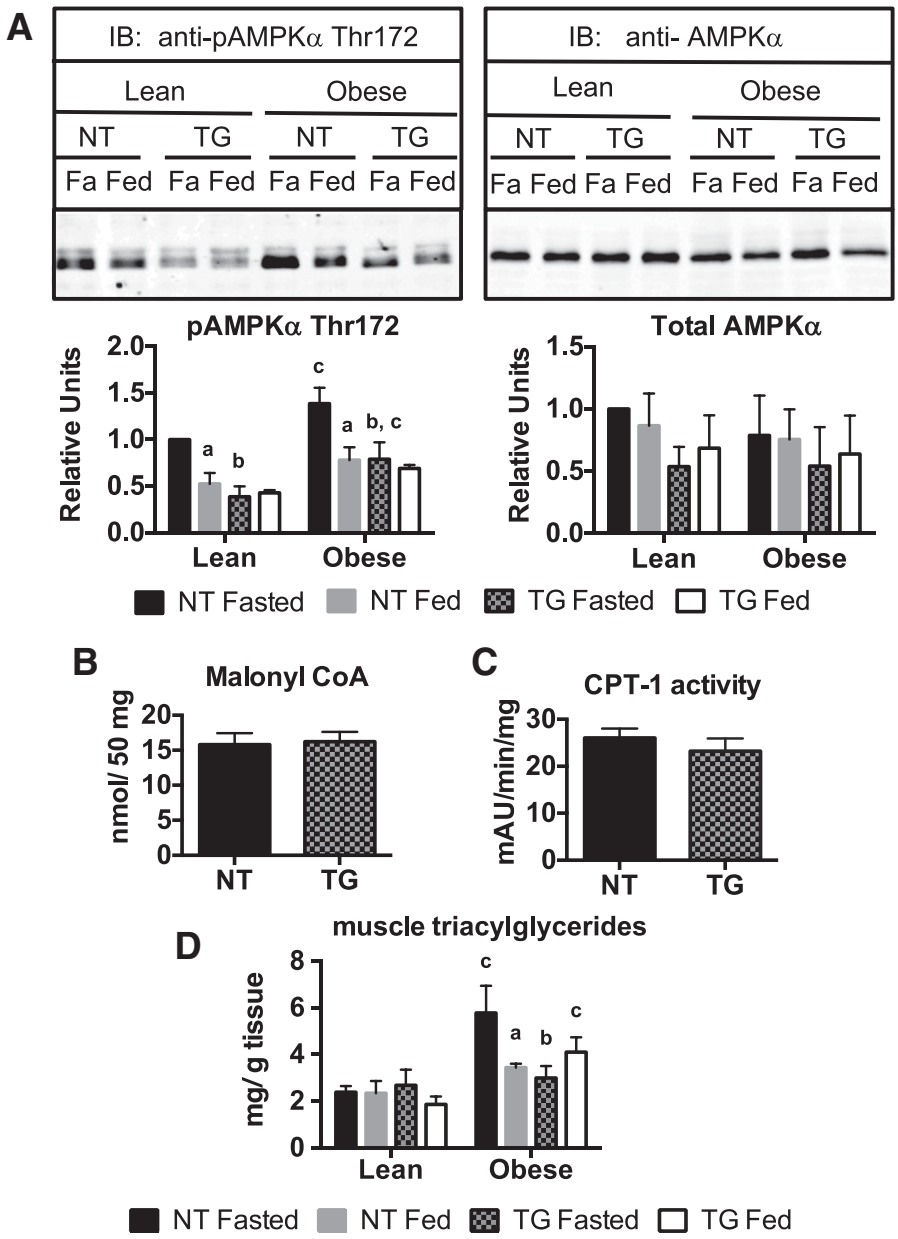

Figure 8—Skeletal muscle AMPK activation, malonyl CoA levels, CPT-1 activity, and TAGs in fasted (Fa) and fed NT and hGLUT4 TG mice fed a CD (Lean) or an HFD (Obese) for 5 weeks. *A*: Representative Western blot analysis and quantification of immunoblots (IB) for phospho-AMPK and total AMPK levels from whole-cell skeletal muscle extracts. Data are the mean and SEM of the relative densitometry units for analysis of three independent muscle extracts for each group. Malonyl CoA levels (*B*), CPT-1 activity (*C*), and muscle triacylglyceride levels (*D*) are all the mean and SEM for four independent measurements. Data for phospho-AMPK and total AMPK and triacylglycerides were analyzed by two-way ANOVA. Pairwise comparisons of 95% CIs established significant differences ($P < 0.05$) between groups. The letter "a" designates a significant difference due to nutritional state (fasted or fed) for a given strain (NT or TG) or body mass (Lean or Obese). The letter "b" designates a significant difference due to strain for a given nutritional state or body mass. The letter "c" indicates a significant difference due to body mass for a given nutritional state or strain. Data for malonyl CoA and CPT-1 activity were analyzed by two-tailed *t* test.

to increased levels of malonyl CoA (Fig. 8*B*) or decreased CPT-1 activity (Fig. 8*C*).

Alternatively, the decrease in obesity-induced production of long-chain acyl carnitines in the presence of the TG could have resulted from the decreased availability of liberated fatty acids due to reduced muscle triacylglycerol (TAG) stores in TG mice. To test this, we measured muscle TAG levels. Obesity increased fasting levels, but not fed levels of muscle TAGs in NT mice. The presence of the TG reduced the fasted TAG levels in obese mice (Fig. 8*B*). These data support the idea that the presence of the TG in obese mice lowers muscle acyl carnitine production and relieves nutrient stress via decreased AMPK activation and reduced muscle TAG accumulation, likely through decreased TAG transport into muscle.

DISCUSSION

The results of our experiments reveal that increased GLUT4-dependent glucose flux has profound effects on a variety of intermediary metabolites and key mitochondrial enzymes. Despite the decrease in key mitochondrial enzymes, we observed no differences in mitochondrial area or number (Fig. 2). We did not assess markers of mitochondrial dynamics, and it is possible that mitochondrial enzymes were reduced as a result of increased mitochondrial turnover. The presence of the GLUT4 TG was associated with a reduced TCA intermediate pool size that was likely due to changes in the rates of anaplerosis and cataplerosis in skeletal muscle. Glutamate oxidation in fed TG mice was reduced, which is consistent with the decreased levels of α-KG in the fed state. The TG did not globally suppress anaplerosis because PCC-dependent anaplerosis was unaffected by genotype (Fig. 2). Although PC-dependent respiration was decreased in fed TG muscle (Fig. 2), this was likely due to the decreased production of acetyl CoA by PDH activity in the fed state (Fig. 2*E*).

There was a significant effect of genotype on amino acid metabolism in skeletal muscle. Skeletal muscle is an important site of amino acid metabolism. After consuming a protein meal, BCAAs are released from the splanchnic circulation, and taken up by skeletal muscle and adipose tissue, where they are further metabolized (28,29). The BCAA amino acids undergo transamination with α-KG as the acceptor to produce Glu and a branched-chain α-keto acid. The increased levels of BCAAs and decreased levels of Glu/Gln and α-KG in TG mice (Figs. 5 and 7) suggest a reduced overall BCAA transamination. Importantly, the elevation in BCAA levels is accompanied by increased abundance of phosphorylated (inactive) BCKDH, further supporting reduced catabolism of BCAA in TG mouse skeletal muscle.

In contrast to BCAA, Ala and Gln are released from skeletal muscle after a protein meal and are taken up by the splanchnic circulation (29,30). Our data suggest that increased GLUT4-dependent glucose flux in both lean and obese mice favors the production of Ala, Gly, and Ser (synthesized from glycolytic intermediates) at the expense of Glu/Gln production (Fig. 4). Increased Gly levels may provide an additional role for protection against metabolic disease by providing the liver with glycine for conjugation and excretion of acyl groups derived from BCAA α-keto acids, a known risk factor for insulin resistance (24,31). This is consistent with a recent publication (32) indicating that reduced skeletal muscle Gly levels were associated with decreased acylglycine conjugates in the urine and insulin sensitivity in Zucker fatty rats. It is unlikely that increased glucogenic amino acids promote protein accretion because there is no TG-dependent increase in 4-EBP1 hyperphosphorylation, and lean body mass is not different when comparing lean or obese NT and TG mice (Fig. 5) (5).

The results of our experiments support the hypothesis that increased GLUT4-dependent glucose flux reduced nutrient stress in obese TG mice (Fig. 7*A*). The accumulation of long-chain acyl carnitines is an accepted biomarker of nutrient stress in obese skeletal muscle (26). There are several potential explanations for how increased GLUT4-dependent glucose transport may be reducing nutrient stress through decreasing the level of long-chain acyl carnitines in obese mice in the fasted state. This could occur via decreased acyl carnitine synthesis or increased acyl carnitine oxidation. Palmitoylcarnitine oxidation was not increased in TG mitochondria (Fig. 2*D*), indicating that oxidation was not increased. The capacity for superoxide anion production was also unchanged (Fig. 2*E*), indicating that this was not a mechanism for reducing nutrient stress. CPT-1 activity and malonyl CoA levels were also unaffected by the TG, which indicated that rates of acylcarnitine synthesis were not changed. There was, however, a significant reduction in muscle TAG levels in obese TG mice compared with their NT counterparts. Thus, we suggest that fasted, obese TG mice have less fatty acid immediately available from lipolysis for long-chain acyl carnitine production. This did not result in a decreased energy charge because phospho-AMPK levels were lower in fasted, obese TG mouse muscle.

Previously, we showed that TG mice exhibited no increase in *srebp-1c* mRNA expression in response to refeeding, suggesting that de novo lipogenesis might be reduced (5). We hypothesize that the increased glucose uptake in muscle tissues, and increased production of Ala reduced the overall level of insulin secretion. Chronically reduced insulin levels could account for decreased lipogenic gene expression in TG mice. This mechanism could explain how increased GLUT4-dependent glucose flux in the periphery may improve hepatic insulin sensitivity in obese animals (5,33). Antidiabetic therapies that target increased glucose uptake in skeletal muscle would, likely, be highly effective.

Funding. This work was supported by National Institutes of Health/National Institute of Diabetes and Digestive and Kidney Diseases grants DK-58398 (C.B.N.) and DK-081545 (A.L.O.).

Duality of Interest. No potential conflicts of interest relevant to this article were reported.

Author Contributions. J.M.G. wrote the manuscript and researched data. O.I., R.M.J., B.A.G., P.W., S.M., R.Q., H.V.R., and K.M.H. researched the data. C.B.N. and A.L.O. conceived the project, oversaw data collection and analysis, contributed to the writing of the manuscript, and reviewed and edited the manuscript. A.L.O. is the guarantor of this work and, as such, had full access to all the data in the study and takes responsibility for the integrity of the data and the accuracy of the data analysis.

Prior Presentation. Parts of this study were presented in abstract form at the 76th Scientific Sessions of the American Diabetes Association, New Orleans, LA, 10–14 June 2016.

References

1. Kahn SEJB, Buse JB. Medications for type 2 diabetes: how will we be treating patients in 50 years? Diabetologia 2015;58:1735–1739

2. Nolan CJ, Ruderman NB, Kahn SE, Pedersen O, Prentki M. Insulin resistance as a physiological defense against metabolic stress: implications for the management of subsets of type 2 diabetes. Diabetes 2015;64:673–686

3. Brüning JC, Michael MD, Winnay JN, et al. A muscle-specific insulin receptor knockout exhibits features of the metabolic syndrome of NIDDM without altering glucose tolerance. Mol Cell 1998;2:559–569
4. Wojtaszewski JFP, Higaki Y, Hirshman MF, et al. Exercise modulates postreceptor insulin signaling and glucose transport in muscle-specific insulin receptor knockout mice. J Clin Invest 1999;104:1257–1264
5. Atkinson BJ, Griesel BA, King CD, Josey MA, Olson AL. Moderate GLUT4 overexpression improves insulin sensitivity and fasting triglyceridemia in high-fat diet-fed transgenic mice. Diabetes 2013;62:2249–2258
6. Gibbs EM, Stock JL, McCoid SC, et al. Glycemic improvement in diabetic db/db mice by overexpression of the human insulin-regulatable glucose transporter (GLUT4). J Clin Invest 1995;95:1512–1518
7. Herman MA, Peroni OD, Villoria J, et al. A novel ChREBP isoform in adipose tissue regulates systemic glucose metabolism. Nature 2012;484:333–338
8. Shepherd PR, Gnudi L, Tozzo E, Yang H, Leach F, Kahn BB. Adipose cell hyperplasia and enhanced glucose disposal in transgenic mice overexpressing GLUT4 selectively in adipose tissue. J Biol Chem 1993;268:22243–22246
9. Treadway JL, Hargrove DM, Nardone NA, et al. Enhanced peripheral glucose utilization in transgenic mice expressing the human GLUT4 gene. J Biol Chem 1994;269:29956–29961
10. Tsao TS, Stenbit AE, Li J, et al. Muscle-specific transgenic complementation of GLUT4-deficient mice. Effects on glucose but not lipid metabolism. J Clin Invest 1997;100:671–677
11. Shulman RG, Bloch G, Rothman DL. In vivo regulation of muscle glycogen synthase and the control of glycogen synthesis. Proc Natl Acad Sci U S A 1995; 92:8535–8542
12. Brozinick JT Jr, Yaspelkis BB 3rd, Wilson CM, et al. Glucose transport and GLUT4 protein distribution in skeletal muscle of GLUT4 transgenic mice. Biochem J 1996;313:133–140
13. Hansen PA, Gulve EA, Marshall BA, et al. Skeletal muscle glucose transport and metabolism are enhanced in transgenic mice overexpressing the Glut4 glucose transporter. J Biol Chem 1995;270:1679–1684
14. Liu M-L, Gibbs EM, McCoid SC, et al. Transgenic mice expressing the human GLUT4/muscle-fat facilitative glucose transporter protein exhibit efficient glycemic control. Proc Natl Acad Sci U S A 1993;90:11346–11350
15. Olson AL, Liu M-L, Moye-Rowley WS, Buse JB, Bell GI, Pessin JE. Hormonal/metabolic regulation of the human GLUT4/muscle-fat facilitative glucose transporter gene in transgenic mice. J Biol Chem 1993;268:9839–9846
16. Olson ALJE, Pessin JE. Transcriptional regulation of the human GLUT4 gene promoter in diabetic transgenic mice. J Biol Chem 1995;270:23491–23495
17. Jang YC, Lustgarten MS, Liu Y, et al. Increased superoxide in vivo accelerates age-associated muscle atrophy through mitochondrial dysfunction and neuromuscular junction degeneration. FASEB J 2010;24:1376–1390
18. Muller FL, Song W, Jang YC, et al. Denervation-induced skeletal muscle atrophy is associated with increased mitochondrial ROS production. Am J Physiol Regul Integr Comp Physiol 2007;293:R1159–R1168
19. Davis EJ, Spydevold O, Bremer J. Pyruvate carboxylase and propionyl-CoA carboxylase as anaplerotic enzymes in skeletal muscle mitochondria. Eur J Biochem 1980;110:255–262
20. Matsuzaki S, Humphries KM. Selective inhibition of deactivated mitochondrial complex I by biguanides. Biochemistry 2015;54:2011–2021
21. Vadvalkar SS, Baily CN, Matsuzaki S, West M, Tesiram YA, Humphries KM. Metabolic inflexibility and protein lysine acetylation in heart mitochondria of a chronic model of type 1 diabetes. Biochem J 2013;449:253–261
22. Humphries KMLI, Szweda LI. Selective inactivation of alpha-ketoglutarate dehydrogenase and pyruvate dehydrogenase: reaction of lipoic acid with 4-hydroxy-2-nonenal. Biochemistry 1998;37:15835–15841
23. An J, Muoio DM, Shiota M, et al. Hepatic expression of malonyl-CoA decarboxylase reverses muscle, liver and whole-animal insulin resistance. Nat Med 2004;10:268–274
24. Newgard CB, An J, Bain JR, et al. A branched-chain amino acid-related metabolic signature that differentiates obese and lean humans and contributes to insulin resistance. Cell Metab 2009;9:311–326
25. Griesel BA, Weems J, Russell RA, Abel ED, Humphries K, Olson AL. Acute inhibition of fatty acid import inhibits GLUT4 transcription in adipose tissue, but not skeletal or cardiac muscle tissue, partly through liver X receptor (LXR) signaling. Diabetes 2010;59:800–807
26. Koves TR, Ussher JR, Noland RC, et al. Mitochondrial overload and incomplete fatty acid oxidation contribute to skeletal muscle insulin resistance. Cell Metab 2008;7:45–56
27. Seiler SE, Martin OJ, Noland RC, et al. Obesity and lipid stress inhibit carnitine acetyltransferase activity. J Lipid Res 2014;55:635–644
28. Herman MA, She P, Peroni OD, Lynch CJ, Kahn BB. Adipose tissue branched chain amino acid (BCAA) metabolism modulates circulating BCAA levels. J Biol Chem 2010;285:11348–11356
29. Wahren J, Felig P, Hagenfeldt L. Effect of protein ingestion on splanchnic and leg metabolism in normal man and in patients with diabetes mellitus. J Clin Invest 1976;57:987–999
30. Garber AJ, Karl IE, Kipnis DM. Alanine and glutamine synthesis and release from skeletal muscle. I. Glycolysis and amino acid release. J Biol Chem 1976; 251:826–835
31. Glynn EL, Piner LW, Huffman KM, et al. Impact of combined resistance and aeorbic exercise training on branched-chain amino acid turnover, glycine metabolism and insulin sensitivity in overweight humans. Diabetologia 2015;58: 2324–2335
32. White PJ, Lapworth AL, An J, et al. Branched-chain amino acid restriction in Zucker-fatty rats improves muscle insulin sensitivity by enhancing efficiency of fatty acid oxidation and acyl-glycine export. Mol Metab 2016;5: 538–551
33. Berglund ED, Li CY, Ayala JE, McGuinness OP, Wasserman DH. Regulation of endogenous glucose production in glucose transporter 4 over-expressing mice. PLoS One 2012;7:e52355